

Fabrication of high-strain rate superplastic yttria-doped zirconia polycrystals by adding manganese and aluminum oxides

Yoshio Sakka*, Tatsunori Ishii, Tohru S. Suzuki, Koji Morita, Keiji Hiraga

National Institute for Materials Science, 1-2-1, Sengen, Tsukuba, Ibaraki, Japan

Abstract

Conventional superplastic ceramics have been established at temperatures over 1400 °C with a slower deformation velocity of about 10^{-4} (s⁻¹). For the application of superplasticity to the manufacturing process, however, high-strain rate deformation velocity of around 10^{-2} /s⁻¹ is necessary. We have reported that alumina addition to 3YTZ (3 mol.% Y₂O₃ doped ZrO₂) is effective in the enhanced ductility. The purpose of this study is to fabricate high-strain rate superplastic 3YTZ by adding manganese and aluminium oxides. Dense and fine-grained 3YTZ systems were obtained by slip casting and low temperature sintering. Manganese and aluminium oxides added 3YTZ showed a maximum tensile ductility of about 600% at 1450 °C at a strain rate of 1.2×10^{-2} s⁻¹.

© 2003 Elsevier Ltd. All rights reserved.

Keywords: Al₂O₃; Colloidal processing; Grain growth; Mn₃O₄; Superplasticity; ZrO₂

1. Introduction

Superplasticity provides the possibility of the high-temperature deformation processing of dense ceramics and has the advantages of sharper formability with better dimensional accuracy. Superplastic ceramics have been widely studied,^{1–11} since superplasticity was first reported in 1986 by Wakai et al.¹ However, superplastic ceramics were only formed at relatively low-strain rates around 10^{-4} s⁻¹ and at higher temperatures above 1400 °C. Recently, we have reported that the deformation rate was enhanced by adding small amount of Al₂O₃ to the 3YTZ (3 mol.% Y₂O₃ doped ZrO₂) system.⁸ This is explained by the enhancement of cation diffusion and homogeneous fine-grained microstructure. The objective of this study is to fabricate more excellent superplastic ceramics by adding Al₂O₃ and Mn₃O₄ to 3YTZ. Here, Mn₃O₄ was added to enhance the cation diffusion of the 3YTZ system, which is expected by the fact that adding Mn₃O₄ enhance the densification of 3YTZ.

To achieve superplasticity, fine-grain size, homogeneous microstructure and high density are necessary.⁷ In order to obtain a fine-grained microstructure after sintering, fine particles must be used. However, fine particles tend to spontaneously agglomerate due to van

der Waals forces. The agglomerated particles form large pores and a high temperature is necessary to eliminate the pores and form dense bodies. Colloidal processing helps to prevent the agglomeration of fine particles and allow the particle dispersion to be controlled during powder processing.⁷ In this study, dispersed aqueous suspensions of 3YTZ, Al₂O₃ and Mn₃O₄ fine particles are consolidated by slip casting. Since the compact have a narrow pore size distribution and are dense, fine-grained and dense sintered specimens are obtained by low temperature sintering. The fine-grained 3YTZ ceramics with added Al₂O₃ and Mn₃O₄ shows high-strain rate superplasticity.

2. Experimental procedure

The raw powders of 3 mol.% Y₂O₃ doped tetragonal ZrO₂ (3YTZ) and 0.3 mol.% Al₂O₃ added 3YTZ (3YTZE) used in this study were produced by Tosoh, and Mn₃O₄ by Nanotek. Average particles sizes of the 3YTZ and 3YTZE powders were 70 nm, and Mn₃O₄ powder was 30 nm. Long range segregation caused by the difference in the particle size and density during slip casting is prevented if the solid content of the suspension is more than 30 vol%.⁷ Therefore, aqueous suspensions containing 30vol% solids were prepared for the composition in the range of 0–0.5 mol.% Mn₃O₄ addition to 3YTZ and 3YTZE.

* Corresponding author.

E-mail address: sakka.yoshio@nims.go.jp (Y. Sakka).

Re-dispersion is necessary to properly disperse a mixture of fine particles because of their agglomeration. The suspensions were ultrasonicated to homogeneously disperse 3YTZ, 3YTZE and Mn_3O_4 particles (20 kHz, 160 kW for 10 min).¹² Sufficient amount of polyelectrolyte (ammonium polyacrylate; Toa gohsei, ALON A-6114) was added to maintain the particle dispersion. Here, the appropriate amount of polyelectrolyte was determined by the amount that produced the minimum suspension viscosity. After evacuation in a desiccators to eliminate air bubbles, the suspension was consolidated by slip casting. The green compacts obtained by the slip casting were further treated by cold isostatic pressing (CIP) at 400 MPa for 10 min. Sintering was conducted at 1100, 1200 and 1300 °C for 2 h in air. The density was measured by Archimedes' method. The microstructures of the sintered specimens were observed by SEM on polished and thermally etched surfaces. The grain growth experiments were conducted in the temperature range of 1450–1600 °C with annealing times of 5–75 h for the dense samples of undoped and 0.5 mol.% Mn_3O_4 added 3YTZ and 3YTZE which had been sintered 1300 °C for 2 h. The average grain sizes were measured by the linear intercept method. Tensile tests were conducted with an Instron-type testing machine for the sample sintered at 1300 °C for 2 h with gauge dimensions of 7(length)×3(width)×2(thickness) mm in a vacuum.

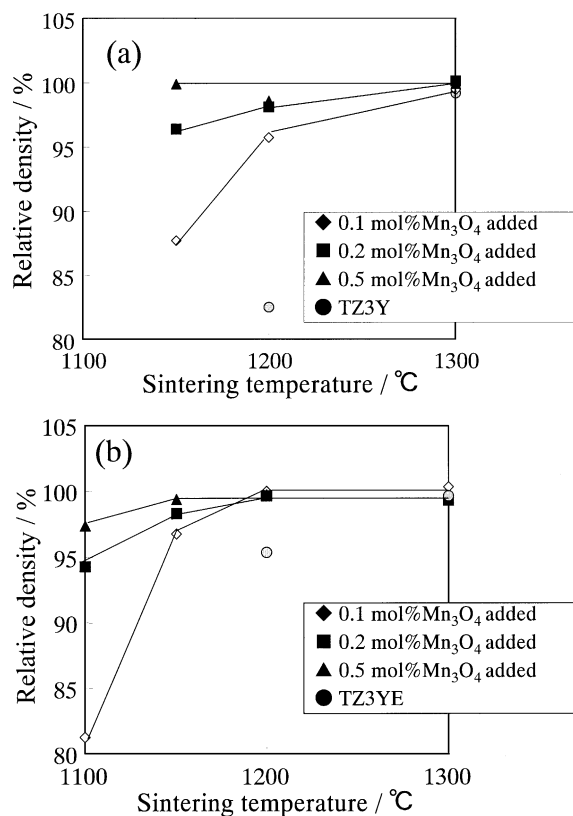


Fig. 1. Relative density of the sample (a) Mn_3O_4 added TZ3Y and (b) Mn_3O_4 added TZ3YE after sintering at fixed temperatures for 2 h.

3. Results and discussion

Fig. 1 shows the densities of the Mn_3O_4 added 3YTZ and 3YTZE sintered at fixed temperatures for 2 h. Significant enhancement of densification is observed by Mn_3O_4 addition. The density of undoped 3YTZ sintered at 1300 °C is only 82%. However, that of 0.1 mol.% Mn_3O_4 added 3YTZ exceeds 95% and that increases with increase of Mn_3O_4 addition. Moreover, the Al_2O_3 addition (3YTZE) in Fig. 1(b), further enhancement of low temperature densification is observed. For example, the density of Al_2O_3 added 3YTZ (3YTZE) sintered at 1300 °C exceeds 95% and 0.1 mol.% Mn_3O_4 addition to 3YTZE results in full density. Fig. 2 shows typical SEM images of the polished and thermally etched 0.2 mol.% Mn_3O_4 added 3YTZ, and 0.2 mol.% Mn_3O_4 added 3YTZE sintered at 1300 °C for 2 h. It is seen that fine-grain size and dense bodies were obtained by this method.

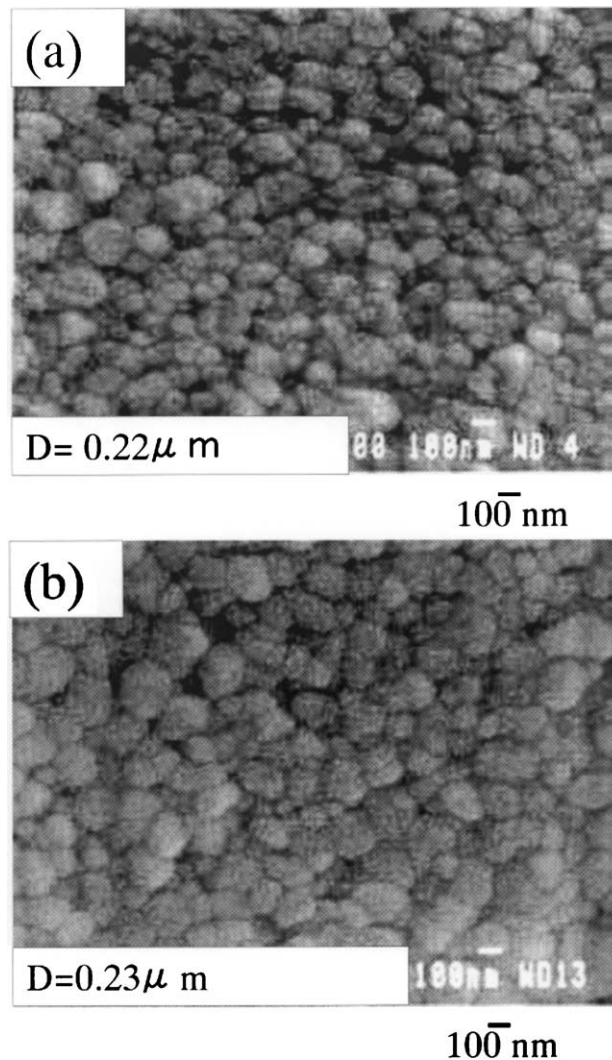


Fig. 2. SEM photographs of (a) 0.2 mol.% Mn_3O_4 added TZ3Y and (b) 0.2 mol.% Mn_3O_4 added TZ3YE sintered at 1200 °C for 2 h.

In this study, sintering condition of 1300 °C for 2 h was used for the static grain growth experiments and tensile tests to examine all the samples with full density. The static grain growths of 3YTZ, 0.3 mol.% Al_2O_3 added 3YTZ (3YTZE), 0.5 mol.% Mn_3O_4 added 3YTZ, and 0.5 mol.% Mn_3O_4 added 3YTZE were analyzed by the following equation.

$$d_s^r - d_0^r = k \cdot t, \quad (1)$$

where r is the grain growth exponent, d_s is grain size after annealing time t (s), and k is the rate constant. Fig. 3 shows that the static grain growth followed $r=3$, that is, the grain growth is controlled by lattice diffusion. Fig. 4 shows the Arrhenius plots of the grain growth rates. The activation energies of the grain growth rates of all samples are also shown. The activation energy of 3YTZ (554 kJ/mol) corresponds to the previously reported one.¹³ The grain growth rate increased by adding Al_2O_3 and Mn_3O_4 in 3YTZ. Since the cation diffusion in the zirconia systems is much smaller than the oxygen diffusion,^{14,15} the grain growth was controlled by cation diffusion. Therefore, it is con-

cluded that cation diffusion is enhanced by adding Al_2O_3 and Mn_3O_4 to 3YTZ.

Fig. 5 illustrates that the stress-strain curves of Mn_3O_4 and/or Al_2O_3 added 3YTZ at a constant strain rate of $1.2 \times 10^{-2} \text{ s}^{-1}$ at 1450 °C. It is seen that 0.2 mol.% Mn_3O_4 added 3YT doesn't show high-strain rate superplasticity but 0.3 mol.% added TZ3Y does. Moreover, co-adding Al_2O_3 and Mn_3O_4 in 3YTZ showed excellent superplasticity. Fig. 6 shows examples before and after deformation of 0.2 mol.% Mn_3O_4 added 3YTZE, where the high-strain rate ($1.2 \times 10^{-2} \text{ s}^{-1}$) and large elongation (600%) was realized.

To determine the high-deformation rate mechanism, the strain rate ($\dot{\epsilon}$) is analyzed by the following equation.

$$\dot{\epsilon} = A \sigma^n \exp\left(-\frac{Q}{RT}\right), \quad (2)$$

where A is a constant, n is the stress exponent, Q is the deformation activation energy, R is the gas constant, and T is the absolute temperature. To obtain the n value, tensile tests were conducted at strain rates from 7.1×10^{-3} to $4.8 \times 10^{-2} \text{ s}^{-1}$ and at a constant tempera-

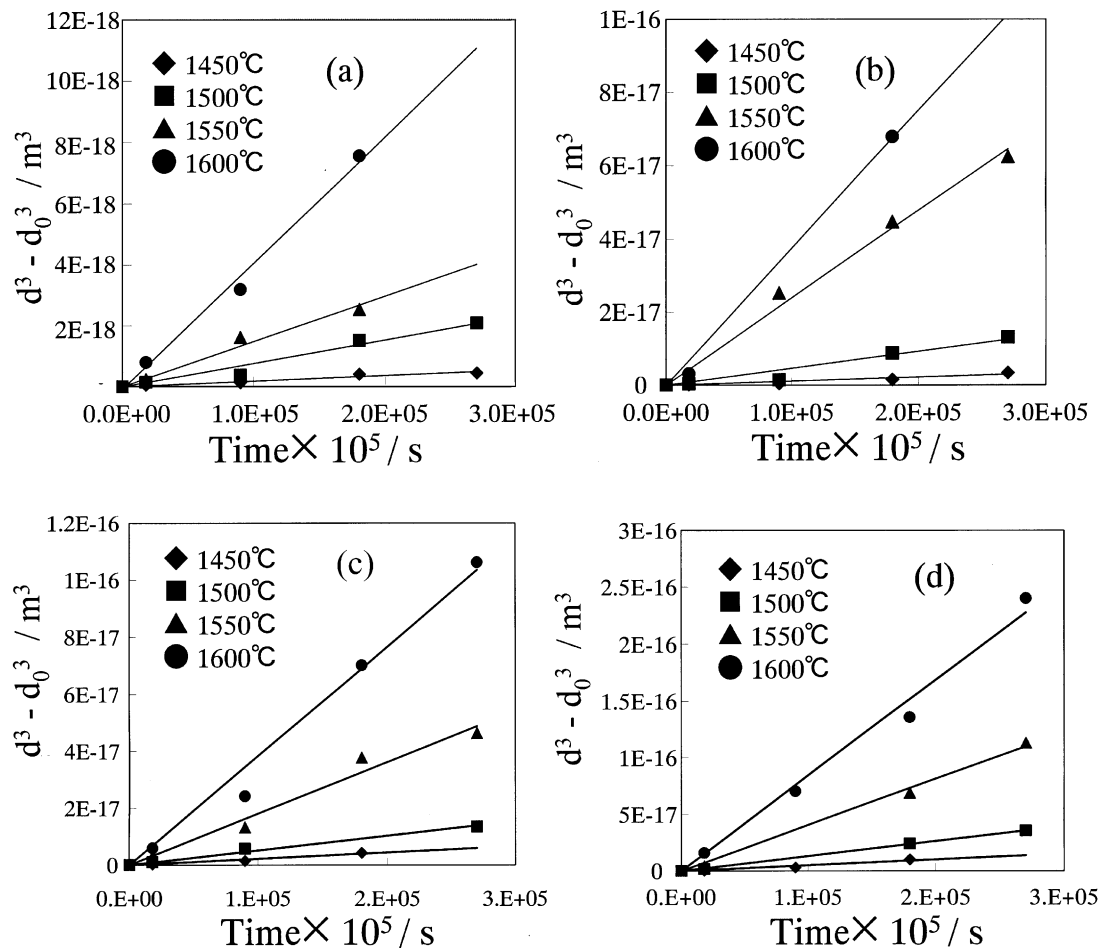


Fig. 3. Grain growth in 3YTZ systems: (a) undoped 3YTZ, (b) 0.3 mol.% Al_2O_3 added 3YTZ, (c) 0.5 mol.% Mn_3O_4 added 3YTZ, (d) 0.5 mol.% Mn_3O_4 added 3YTZE.

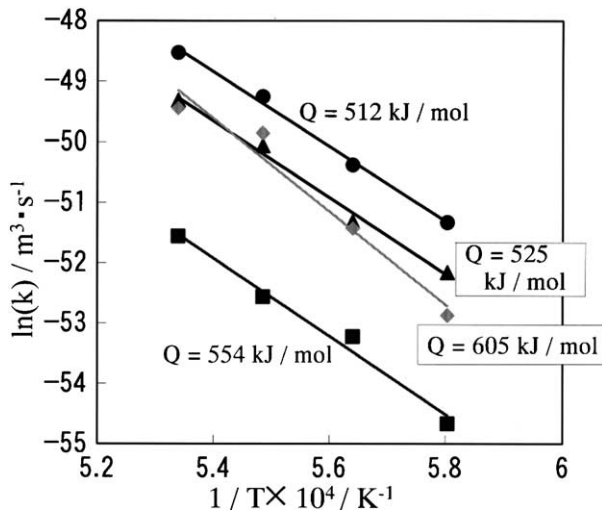


Fig. 4. Arrhenius plots and activation energies of the grain growth rates. ■: 3YTZ, ◆: 0.3 mol.% Al_2O_3 added 3YTZ, ▲: 0.5 mol.% Mn_3O_4 added 3YTZ, ●: 0.5 mol.% Mn_3O_4 added 3YTZE.

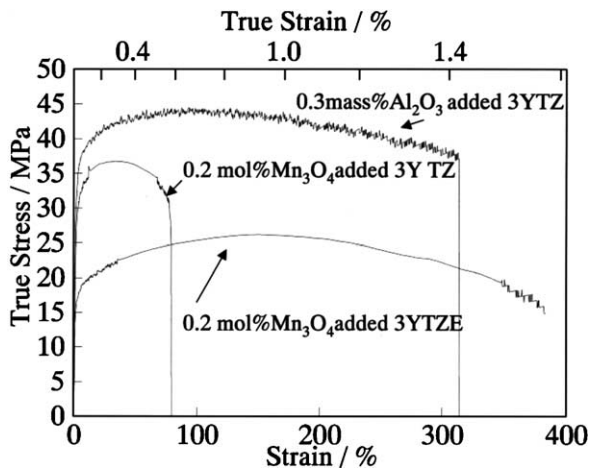


Fig. 5. Stress vs strain curves of 0.2 mol.% Mn_3O_4 added 3YTZ, 0.3 mol.% Al_2O_3 added 3YTZ and 0.2 mol.% Mn_3O_4 added 3YTZE at an initial strain rate of $1.2 \times 10^{-2} \text{ s}^{-1}$ at 1450°C .

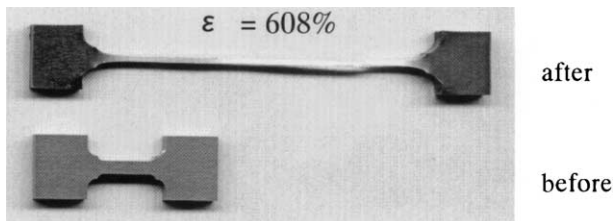


Fig. 6. Macroscopic view of tensile specimens before and after tensile deformation for 0.2 mol.% Mn_3O_4 added 3YTZE at an initial strain rate of $1.2 \times 10^{-2} \text{ s}^{-1}$ at 1450°C .

ture of 1450°C . The $\ln \dot{\epsilon}$ vs. $\ln \sigma$ plots are shown in Fig. 7. Here, the data of 3YTZ that normalized the initial grain size at $0.40 \mu\text{m}$ are also shown. It is noted that the plots of all samples were expressed as a single line up to the high-deformation rate region, and the

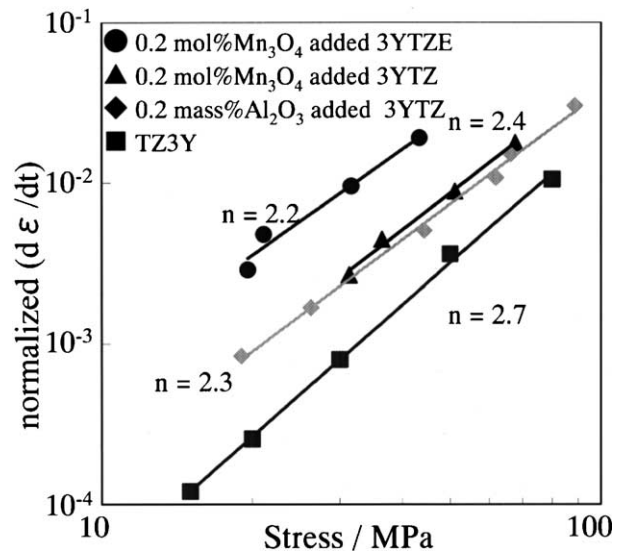


Fig. 7. The $\ln \dot{\epsilon}$ vs. $\ln \sigma$ plots.

n -value is calculated to be in the range of 2.2–2.7. It is seen that addition of Al_2O_3 and/or Mn_3O_4 decreases the deformation stress and increases the strain rate remarkably. Recently, we have reported that the deformation rate of 3YTZ in the high stress region is controlled by the recovery of intragranular dislocation,^{9,11} therefore the accommodation process is controlled by the cation lattice diffusion. If this mechanism is applicable in the present Al_2O_3 and/or Mn_3O_4 added 3YTZ, the result also indicates that the cation diffusion is enhanced by adding Al_2O_3 and Mn_3O_4 . To clarify the mechanism, however, determination of the solubility of Al_2O_3 and Mn_3O_4 to 3YTZ, precise observation of inter- and intra-grain, and further deformation tests are needed.

As stated above, the grain growth rate is enhanced by adding Al_2O_3 and Mn_3O_4 . Therefore, a large grain growth occurred during the tensile test, and the flow stress increased. This seems to be a disadvantage for the superplasticity. Nevertheless, it is confirmed that the tensile ductility is improved by adding Al_2O_3 and Mn_3O_4 at the high strain rate of $1.2 \times 10^{-2} \text{ s}^{-1}$. By adding Al_2O_3 and Mn_3O_4 , the grain growth is enhanced and the plastic flow is disturbed. On the other hand, the accommodation process is also enhanced due to the enhancement of cation diffusion. Hence, the relationship between grain growth and the accommodation process are trade offs. In this case, the second one is more effective, and high strain rate superplasticity is achieved for the homogeneous, fine-grained and dense samples.

4. Conclusions

1. The homogeneous, dense and fine-grained sintered bodies of Al_2O_3 and/or Mn_3O_4 dispersed 3YTZ were obtained by colloidal processing.

2. The grain growth of undoped 3YTZ and Al_2O_3 and/or Mn_3O_4 added 3YTZ were rate-controlled by cation lattice diffusion, and the grain growth rate was enhanced by adding Al_2O_3 and/or Mn_3O_4 .
3. The high-strain rate superplasticity of about 600% was achieved for 0.3 mol.% Al_2O_3 and 0.2 mol.% Mn_3O_4 doped 3YTZ at the strain rate of $1.2 \times 10^{-2} \text{ s}^{-1}$ and at the temperature of 1450 °C.

References

1. Wakai, F., Sakaguchi, S. and Matsuno, Y., Superplasticity of yttria-stabilized ZrO_2 polycrystals. *Adv. Ceram. Mater.*, 1986, **1**, 259–263.
2. Nieh, T. G. and Wadsworth, J., Superplastic behaviour of a fine-grained yttria-stabilized tetragonal zirconia polycrystal (Y-TZP). *Acta Metall. Mater.*, 1990, **38**, 1121–1133.
3. Chokshi, A. H., Superplasticity in fine grained ceramics and ceramic composites: current understanding and future prospects. *Mater. Sci. Eng.*, 1993, **A166**, 119–133.
4. Primdahl, S., Tholen, A. and Langdon, T. G., Microstructural examination of a superplastic yttria-stabilized zirconia: implications for the superplasticity mechanism. *Acta Metall. Mater.*, 1995, **43**, 1211–1218.
5. Kajiwar, K., Yoshizawa, Y. and Sakuma, K., The enhancement of superplastic flow in tetragonal zirconia polycrystals with SiO_2 -doping. *Acta Metall. Mater.*, 1998, **37**, 760–766.
6. Jimenez-Melendo, M., Dominguez-Rodriguez, A. and Bravo-leon, A., Superplastic flow of fine-grained yttria-stabilized zirconia polycrystals: constitutive equation and deformation mechanisms. *J. Am. Ceram. Soc.*, 1998, **81**, 2761–2776.
7. Sakka, Y. and Hiraga, K., Preparation methods and superplastic properties of fine-grained zirconia and alumina based ceramics. *Nippon Kagaku Kaishi*, 1999, 497–506.
8. Suzuki, T. S., Sakka, Y., Nakano, K. and Hiraga, K., Enhanced superplasticity in a alumina-containing zirconia prepared by colloidal processing. *Scripta Mater.*, 2000, **43**, 705–710.
9. Morita, K., Hiraga, K. and Sakka, Y., High temperature deformation of yttria-stabilized tetragonal zirconia. *Mater. Sci. Forum*, 2001, **357–359**, 187–192.
10. Sakka, Y., Suzuki, T. S., Morita, K., Nakano, K. and Hiraga, K., Colloidal processing and superplastic properties of zirconia- and alumina-based nanocomposites. *Scripta Mater.*, 2001, **44**, 2075–2078.
11. Morita, K. and Hiraga, K., Critical assessment of high-temperature deformation and deformed microstructure in high-purity tetragonal zirconia containing 3 mol.% yttria. *Acta Mater.*, 2002, **50**, 1075–1085.
12. Suzuki, T. S., Sakka, Y., Nakano, K. and Hiraga, K., Effect of ultrasonication on the microstructure and tensile elongation of zirconia-dispersed alumina ceramics prepared by colloidal processing. *J. Am. Ceram. Soc.*, 2001, **84**, 2132–2134.
13. Nieh, T. and Wadsworth, J., Dynamic grain growth during superplastic deformation of yttria-stabilized tetragonal zirconia polycrystals. *J. Am. Ceram. Soc.*, 1989, **72**, 1469–1472.
14. Sakka, Y., Oishi, Y. and Ando, K., Zr–Hf interdiffusion in polycrystalline $\text{Y}_2\text{O}_3\text{-(Zr+Hf)O}_2$. *J. Mater. Sci.*, 1982, **17**, 3101–3105.
15. Sakka, Y., Oishi, Y., Ando, K. and Morita, S., Cation interdiffusion and phase stability in polycrystalline tetragonal ceria-zirconia-hafnia solid solution. *J. Am. Ceram. Soc.*, 1991, **74**, 2610–2614.